Validation of a Container Ship Model for Parametric Rolling

Claudio A. Rodríguez

Department of Naval Architecture and Ocean Engineering, LabOceano/COPPE, Federal University of Rio de Janeiro

Christian Holden[1]

Department of Engineering Cybernetics, Norwegian University of Science and Technology

Tristan Perez

Centre for Ships and Ocean Structures (CESOS), Norwegian University of Science and Technology

Ingo Drummen

Centre for Ships and Ocean Structures (CESOS), Norwegian University of Science and Technology

Marcelo A. S. Neves

Department of Naval Architecture and Ocean Engineering, LabOceano/COPPE, Federal University of Rio de Janeiro

Thor I. Fossen

Department of Engineering Cybernetics, Norwegian University of Science and Technology

ABSTRACT

The objective of this work is to formulate a nonlinear, coupled model of a container ship during parametric roll resonance, and to validate the model using experimental data.

KEYWORDS

Ship stability; parametric resonance; non-linear equations; ship motions; roll motion

INTRODUCTION

Parametric resonance is a phenomenon where changes in the model parameters induce a resonance. This is known to occur for the rolling of ships with significant changes of restoring characteristics due to wave passage along the hull and wave excited vertical motions — typical ships affected by this are fishing vessels and container ships. The phenomenon is characteristic when sailing in head or stern seas with wave lengths similar to the ship length, encounter frequency of about twice the roll natural frequency, and wave heights above a ship-dependant threshold value.

Neves and Rodríguez (2005a, b, 2006a) developed a third-order model describing strongly coupled heave, roll and pitch restoring terms via a multivariable Taylor expansion up to the third order. This model has been validated against experimental results for fishing vessels (Neves and Rodríguez, 2005a, b, 2006a).

[1] Corresponding author. E-mail: c.holden@ieee.org

In this work, the proposed model is used to describe the motion of a container ship. The parameters are determined numerically from the vessel loading condition and line drawings An alternative (more accurate) methodology based on the instantaneous determination of the calm water and wave pressure fields, is introduced. This is achieved employing a dedicated panel method code. The fidelity of the container ship model is then assessed using experimental data of a 1:45 scale model of a container vessel with an overall length of 294 m. This vessel has a large, flat, overhanging stern and pronounced bow flare — characteristics representative for modern container vessels, and known to be prone to parametric roll resonance.

The experiments were conducted in a towing tank in head seas regular and irregular waves for different forward speeds and wave heights and frequency. Parametric roll resonance was observed in some runs, but not in others, giving us a wide range of conditions with which to verify the model. Free roll decay tests were also performed in calm water.

MODEL

A linear or non-linear 1DOF model can, in certain cases, capture the rolling of ships. In the case where parametric resonance may occur, however, the nonlinear coupling between pitch, roll and heave are important to understand the phenomenon. This gives rise to the 3DOF model presented in Neves and Rodríguez (2006a):

Let

$$\mathbf{s} = \begin{bmatrix} z(t) & \phi(t) & \theta(t) \end{bmatrix}^T \tag{1}$$

where z is the heave displacement, ϕ is the roll and θ is the pitch angle of the vessel.

This gives a model

$$(\mathbf{M}+\mathbf{A})\ddot{\mathbf{s}} + \mathbf{B}(\dot{\phi})\dot{\mathbf{s}} + \mathbf{c}_r(\mathbf{s},\zeta) = \mathbf{c}_{ext}(\zeta,\dot{\zeta},\ddot{\zeta}) \tag{2}$$

where $\mathbf{M} \in \mathbf{R}^{3\times3}$ is the diagonal rigid body inertia of the vessel. $\mathbf{A} \in \mathbf{R}^{3\times3}$ is the hydrodynamic generalized added mass. $\mathbf{B} \in \mathbf{R}^{3\times3}$ is the hydrodynamic damping, which is non-linear in roll. $\mathbf{c}_\mathbf{r} \in \mathbf{R}^3$ is the non-linear vector of restoring forces and moments, which depends on the relative motions between ship hull and wave elevation $\zeta(t)$. The vector $\mathbf{c}_{ext} \in \mathbf{R}^3$ represents the external wave excitation forces and moments, which change with wave heading, encounter frequency, wave amplitude and time, and it is assumed—for simplicity—to be independent of the state variables $\mathbf{s}$.

Added Mass and Damping

The hydrodynamic mass and damping matrices can be expressed as

$$\mathbf{A} = \begin{bmatrix} Z_{\ddot{z}} & 0 & Z_{\ddot{\theta}} \\ 0 & K_{\ddot{\phi}} & 0 \\ M_{\ddot{z}} & 0 & M_{\ddot{\theta}} \end{bmatrix} \tag{3}$$

$$\mathbf{B} = \begin{bmatrix} Z_{\dot{z}} & 0 & Z_{\dot{\theta}} \\ 0 & K_{\dot{\phi}}(\dot{\phi}) & 0 \\ M_{\dot{z}} & 0 & M_{\dot{\theta}} \end{bmatrix} \tag{4}$$

where all terms except for $K_{\dot{\phi}}$ can be evaluated by means of potential theory. Mathematically, $K_{\dot{\phi}}$ can be approximated as

$$K_{\dot{\phi}}(\dot{\phi})\dot{\phi} = K_{\dot{\phi}}\dot{\phi} + K_{\dot{\phi}|\dot{\phi}|}\dot{\phi}\left|\dot{\phi}\right| \tag{5}$$

This consists of a linear part (potential and linear skin friction) and a nonlinear term (viscous effects). Linear and non-linear coefficients in (5) may be computed using the formulae given in Himeno (1981). Alternatively, the damping can be estimated from data of roll decaying tests at the appropriate forward speed of the vessel.

Non-Linear Restoring Forces and Moments

The vector $\mathbf{c}_r$ of non-linear restoring forces and moments can be approximated as

$$\mathbf{c}_r = \mathbf{c}_r^{(1)} + \mathbf{c}_{r(m)}^{(2)} + \mathbf{c}_{r(w)}^{(2)} + \mathbf{c}_{r(m)}^{(3)} + \mathbf{c}_{r(3)}^{(3)}$$
$$= \begin{bmatrix} Z_r^{(1)} \\ K_r^{(1)} \\ M_r^{(1)} \end{bmatrix} + \begin{bmatrix} Z_{r(m)}^{(2)} + M_{r(w)}^{(2)} \\ K_{r(m)}^{(2)} + M_{r(w)}^{(2)} \\ M_{r(m)}^{(2)} + M_{r(w)}^{(2)} \end{bmatrix} \qquad (6)$$
$$+ \begin{bmatrix} Z_{r(m)}^{(3)} + M_{r(w)}^{(3)} \\ K_{r(m)}^{(3)} + M_{r(w)}^{(3)} \\ M_{r(m)}^{(3)} + M_{r(w)}^{(3)} \end{bmatrix}$$

where indices (1), (2) and (3) respectively refer to first, second and third order terms.

The first order terms correspond to the calm water hydrostatics:

$$Z_r^{(1)} = Z_z z + Z_\theta \theta = \rho g A_0 z - \rho g A_0 x_{f_0} \theta$$
$$K_r^{(1)} = K_\phi \phi = \Delta \overline{\mathrm{GM}} \phi$$
$$M_r^{(1)} = M_z z + M_\theta \theta = -\rho g A_0 x_{f_0} z + \Delta \overline{\mathrm{GM}}_L \theta$$

where ρ is water density, g is the acceleration of gravity, A_0 is the waterplane area, x_{f_0} the longitudinal coordinate of the centroid of the waterplane area, $\overline{\mathrm{GM}}$ is the transverse metacentric height, and $\overline{\mathrm{GM}}_\mathrm{L}$ the longitudinal metacentric height.

Two different effects cause second- and third-order terms: subscripts (m) refer to body motions and (w) to wave effects. Derivations of these actions, based on multivariable Taylor series expansions have been presented in Neves and Rodríguez (2005a, 2006a):

$$Z_{r(m)}^{(2)} = \frac{1}{2}\left(Z_{zz} z^2 + 2 Z_{z\theta} z\theta + Z_{\phi\phi} \phi^2 + Z_{\theta\theta} \theta^2 \right)$$
$$K_{r(m)}^{(2)} = K_{z\phi} z\phi + K_{\phi\theta} \phi\theta$$
$$M_{r(m)}^{(2)} = \frac{1}{2}\left(M_{zz} z^2 + 2 M_{z\theta} z\theta + M_{\phi\phi} \phi^2 + M_{\theta\theta} \theta^2 \right)$$

The second-order restoring forces caused by waves can be written as

$$Z_{r(w)}^{(2)} = Z_{\zeta z}(t) z + Z_{\zeta\theta}(t) \theta$$
$$K_{r(w)}^{(2)} = K_{\zeta\phi}(t) \phi$$
$$M_{r(w)}^{(2)} = M_{\zeta z}(t) z + M_{\zeta\theta}(t) \theta$$

Third order restoring forces due to body motions can be written as

$$Z_{r(m)}^{(3)} = \frac{1}{6}\left(Z_{zzz} z^3 + 3 Z_{zz\theta} z^2 \theta + 3 Z_{z\theta\theta} z\theta^2 + Z_{\theta\theta\theta} \theta^3 + 3 Z_{\phi\phi z} z\phi^2 + 3 Z_{\phi\phi\theta} \phi^2 \theta \right)$$
$$K_{r(m)}^{(3)} = \frac{1}{6}\left(K_{\phi\phi\phi} \phi^3 + 3 K_{zz\phi} z^2 \phi + 3 K_{\theta\theta\phi} \theta^2 \phi + 6 K_{z\phi\theta} z\phi\theta \right)$$
$$M_{r(m)}^{(3)} = \frac{1}{6}\left(M_{zzz} z^3 + 3 M_{zz\theta} z^2 \theta + 3 M_{z\theta\theta} z\theta^2 + M_{\theta\theta\theta} \theta^3 + 3 M_{\phi\phi z} z\phi^2 + 3 M_{\phi\phi\theta} \phi^2 \theta \right)$$

Finally, third order restoring forces due to waves can be written as

$$Z_{r(w)}^{(3)} = Z_{\zeta\zeta z}(t) z + Z_{\zeta zz}(t) z^2 + Z_{\zeta\zeta\theta}(t) \theta + Z_{\zeta z\theta}(t) z\theta + Z_{\zeta\phi\phi}(t) \phi^2 + Z_{\zeta\theta\theta}(t) \theta^2$$
$$K_{r(w)}^{(3)} = K_{\zeta\zeta\phi}(t) \phi + K_{\zeta z\phi}(t) z\phi + K_{\zeta z\theta}(t) \theta$$
$$M_{r(w)}^{(3)} = M_{\zeta\zeta z}(t) z + M_{\zeta zz}(t) z^2 + M_{\zeta\zeta\theta}(t) \theta + M_{\zeta z\theta}(t) z\theta + M_{\zeta\phi\phi}(t) \phi^2 + M_{\zeta\theta\theta}(t) \theta^2$$

Note the strong coupling between all three degrees of freedom. Also note that the time-dependant terms are explicit functions of the wave elevation $\zeta(t)$, and therefore implicit functions of time. Further details and analytical expressions relating the coefficients to the characteristics of the vessel can be found in Neves and Rodríguez (2005a, 2006a). In this paper a more general procedure is introduced for the computation of the *derivatives* of the Taylor series expansions.

Calm Water Derivatives

In equation (6) the terms $c_{r(m)}^{(2)}$ and $c_{r(m)}^{(3)}$ describe the changes in the restoring characteristics of the vessel due to the changes in pressure associated with the bodily motions of the vessel.

It is possible to show that nonlinear hydrostatic actions may be expressed as:

$$Z(z, \phi, \theta) = \rho g (\nabla_1 - \nabla_0)$$

$$K(z,\phi,\theta) = \rho g\left[\nabla_0 z_G \sin\phi + \nabla_1\left(y_{B1}\cos\phi - z_{B1}\sin\phi\right)\right]$$

$$M(z,\phi,\theta) = \rho g\left[\nabla_0 z_G \cos\phi\sin\theta - \nabla_1\left(x_{B1}\cos\theta + y_{B1}\sin\phi\sin\theta + z_{B1}\cos\phi\sin\theta\right)\right]$$

where ∇_0 is the average submerged volume, $\nabla_1(z,\phi,\theta)$ is the instantaneous submerged volume, z_G is the vertical coordinate of centre of gravity and $x_{B1}(z,\phi,\theta)$, $y_{B1}(z,\phi,\theta)$ and $z_{B1}(z,\phi,\theta)$ are the coordinates of instantaneous centroid of ∇_1. These expressions allow the numerical determination of all the calm water derivatives appearing in equation (6). This is achieved by means of suitably discrediting the instantaneous displaced hull for generic displacements $[z,\phi,\theta]$. Tables A1 and A2 in the Appendix show the second and third order coefficients.

Wave Effect Derivatives

The terms $\mathbf{c}^{(2)}_{r(w)}$ and $\mathbf{c}^{(3)}_{r(w)}$ in Equation (6) describe the changes in the restoring characteristics of the vessel due to the cyclic changes in pressure associated with the wave profile moving along the hull.

In regular seas, incident wave elevation can be written as

$$\zeta(x,y,t;\chi) = A_w\cos(kx\cos\chi + ky\sin\chi - \omega_e t) \quad (7)$$

where A_w is wave amplitude, k wave number, χ wave heading and ω_e encounter frequency, and the special coordinates are described relative to an inertial coordinate system traveling with the vessel.

The velocity potential for the undisturbed incident wave is given by

$$\phi_I(x,y,z,t) = \frac{A_w g}{\omega_w}e^{kz}\sin[k(x\cos\chi + y\,\mathrm{sen}\,\chi) - \omega_e t]$$

The first and second order generalized Froude-Krilov forces are:

$$F_j^{FK(1)}(t) = \rho\iint\frac{\partial\phi_I}{\partial t}n_j\,\mathrm{d}S$$

$$F_j^{FK(2)}(t) = \frac{1}{2}\rho\iint(\nabla\phi_I.\nabla\phi_I)n_j\,\mathrm{d}S \quad (8)$$

where n_j is the normal to the hull surface, j = *3*, *4* and *5* for heave, roll and pitch, respectively. After computing the forces for a ship at arbitrary positions, the wave passage derivatives may be obtained according to the expressions given in Tables A3 and A4 in the Appendix.

Since the waves are regular, the coefficients can be described as a sum of a sine and a cosine term. For instance, the second-order term $K_{\zeta\phi}(t)$, which is proportional to wave amplitude, can be written as

$$K_{\zeta\phi}(t) = A_w\left[K_{\zeta\phi c}\cos(\omega_e t) + K_{\zeta\phi s}\sin(\omega_e t)\right] \quad (9)$$

where $K_{\zeta\phi c}$ and $K_{\zeta\phi s}$ are constants.

Similarly, the third-order terms $K_{\zeta z\phi}(t)$ and $K_{\zeta\phi\theta}(t)$ (also proportional to wave amplitude) can be expressed as

$$K_{\zeta z\phi}(t) = A_w\left[K_{\zeta z\phi c}\cos(\omega_e t) + K_{\zeta z\phi s}\sin(\omega_e t)\right]$$

$$K_{\zeta\phi\theta}(t) = A_w\left[K_{\zeta\phi\theta c}\cos(\omega_e t) + K_{\zeta\phi\theta s}\sin(\omega_e t)\right] \quad (10)$$

Note that these two functions represent periodic excitation of roll, and are multiplied with, respectively, $z(t)\phi(t)$ and $\theta(t)\phi(t)$. z and θ are both periodic functions dependent on wave amplitude.

The third-order term $K_{\zeta\zeta\phi}(t)$, proportional to the square of the wave amplitude, can be written as

$$K_{\zeta\zeta\phi}(t) = A_w^2\left[K_{\zeta\zeta\phi 0} + K_{\zeta\zeta\phi c}\cos(2\omega_e t) + K_{\zeta\zeta\phi s}\sin(2\omega_e t)\right] \quad (11)$$

which comprises a constant term plus a super-harmonic of double the encounter frequency.

CHARACTERISTICS OF THE VESSEL

To test the fidelity of the model, numerical simulations were compared to experimental results. The experiments were conducted on a 1:45 scale model of a 294m long container

ship. The main characteristics of the vessel can be found in Table 1.

Table 1: Vessel main characteristics (full scale)

Displacement	76,468,800 kg
Hull length	280.982 m
Hull breadth amidships	32.26 m
Hull draught amidships	11.75 m
Roll radius of gyration	12.234 m
Transverse metacentric height	1.843 m

The ship's stability curve can be seen in Figure 1.

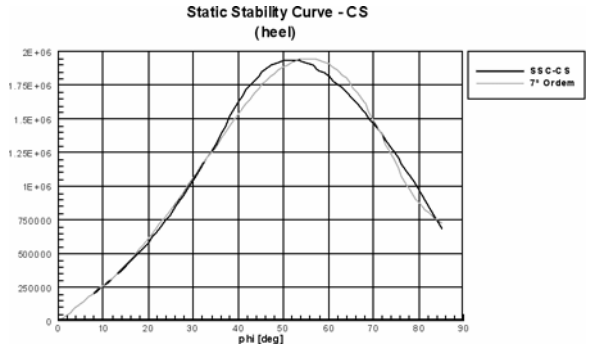

Fig. 1: Static stability curve and the odd seventh-order fit.

TESTED CONDITIONS

In this paper, we consider only the regular wave conditions. A total of 22 tests were performed in regular seas. The test conditions can be seen in Table 2.

The first column is the Froude number. The second column is the encounter frequency. The third column is the ratio of the encounter frequency to the vessel's natural roll frequency. Parametric resonance is known to occur when this is approximately 2. The fourth column is the wave height, and the last column is the test number. The tests were performed in order of increasing test number.

Table 2: Tested conditions

F_n	ω_e	Tuning	H (m)	Test #
0.1035	0.5519	1.85	5	1173
	0.5519	1.85	7	1181
0.1035	0.5677	1.91	5	1175
	0.5677	1.91	7	1183
0.1035	0.5756	1.93	3	1179
0.0879	0.5662	1.90	5	1192
0.0931	0.5723	1.92	5	1193
0.0983	0.5783	1.94	5	1191
			3	1177
0.1035	0.5844	1.96	5	1172
			7	1180
0.1087	0.5904	1.98	5	1184
0.1137	0.5963	2.00	5	1185
0.1189	0.6023	2.02	5	1186
0.1241	0.6084	2.04	5	1187
0.1345	0.6204	2.08	5	1188
0.1397	0.6265	2.10	5	1190
0.1448	0.6324	2.12	5	1189
0.1035	0.5933	1.99	3	1178
0.1035	0.6031	2.03	5	1174
0.1035	0.6231	2.09	5	1176
			7	1182

RESULTS

Some of the results from the experiments, plotted together with the simulation results, can be seen in Figures 2–19. The figures match the order in Table 2, which corresponds to decreasing values of λ / L.

It can be observed that the model provides a good description of the phenomenon for all length ratios; both in terms of roll amplitude and rate of amplification. Conditions with/ without parametric resonance are well modeled, as shown in Figure 20, except for the test cases corresponding to tunings in both extremes of the range of instability for the $\lambda / L = 1.00$ wave condition, at which the bifurcation points are quite sensitive to variation of parameters. It should be noted that the sensitivity of the limits of stability to changes in the system parameters has already been pointed out in Neves and Rodríguez (2006b) in particular with regard to changes in initial conditions.

The differences near the regions of bifurcations defined by limits of stability may be observed in Figure 20, which shows a comparison in the frequency domain of different maximum roll amplitudes for waves of length equal to the ship length and $A_w = 2.5\text{m}$. A condition for $A_w = 3.5\text{m}$ is also included. In Figure 21 we can see the complete numerical mapping of roll amplitudes (indicated by the scaled color variation) for different tunings (or, equivalently, forward speeds) and wave amplitudes for the same $\lambda / L = 1.00$ wave condition.

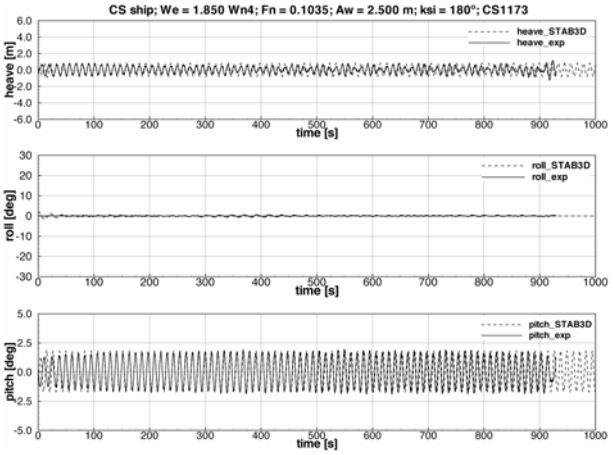

Fig. 2: Exp. 1173 ($\lambda / L = 1.10$). No parametric resonance.

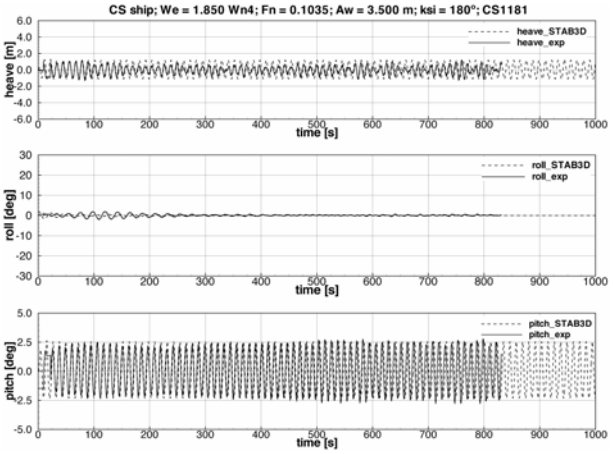

Fig 3: Exp. 1181 ($\lambda / L = 1.10$). No parametric resonance.

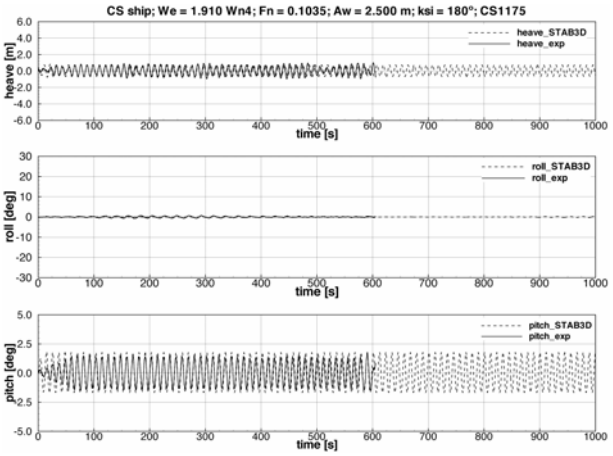

Fig. 4: Exp. 1175 ($\lambda / L = 1.05$). No parametric resonance.

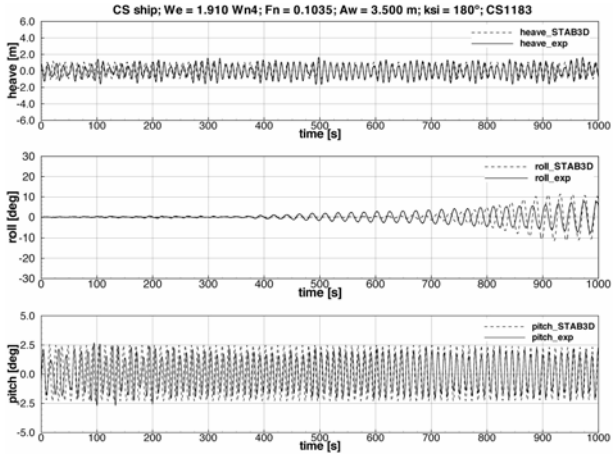

Fig. 5: Exp. 1183 ($\lambda / L = 1.05$). Weak amplification.

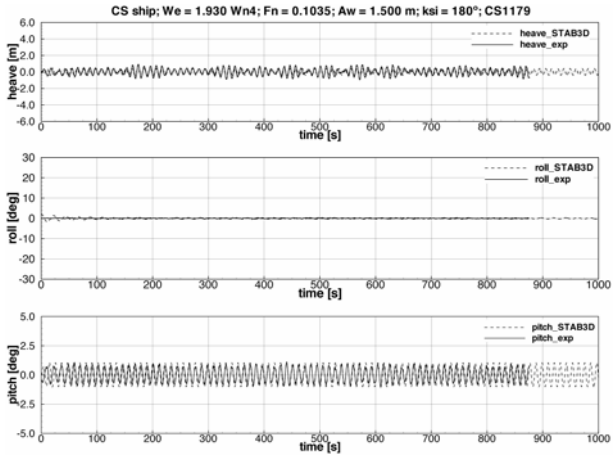

Fig. 6: Exp. 1179 ($\lambda / L = 1.02$). No parametric resonance.

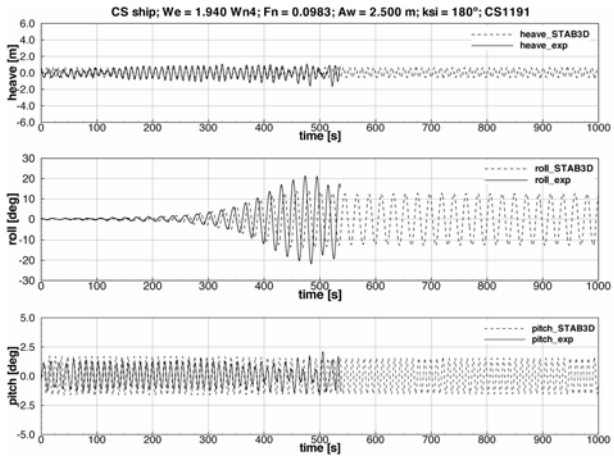

Fig. 7: Exp. 1191 ($\lambda / L = 1.00$). Parametric resonance occurs.

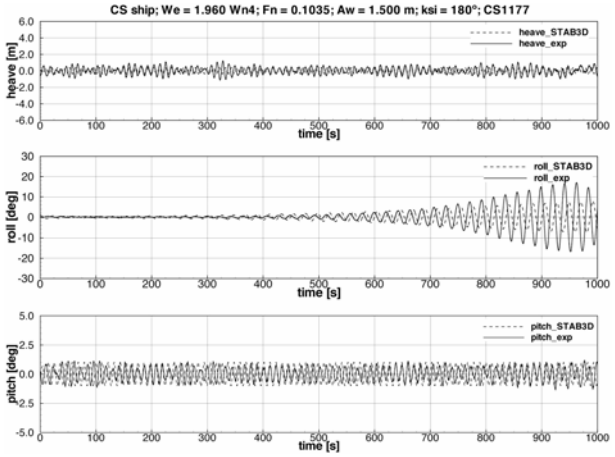

Fig. 8: Exp. 1177 ($\lambda / L = 1.00$). Weak amplification.

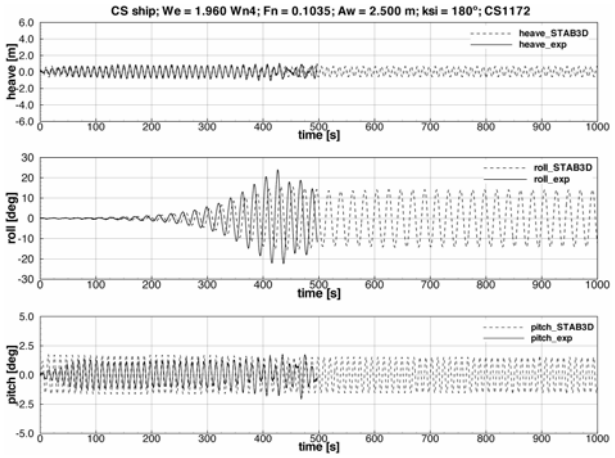

Fig. 9: Exp. 1172 ($\lambda / L = 1.00$). Parametric resonance occurs.

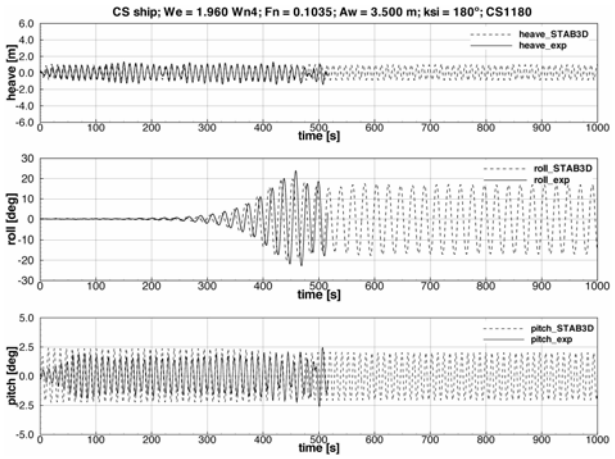

Fig. 10: Exp. 1180 ($\lambda / L = 1.00$). Parametric resonance occurs.

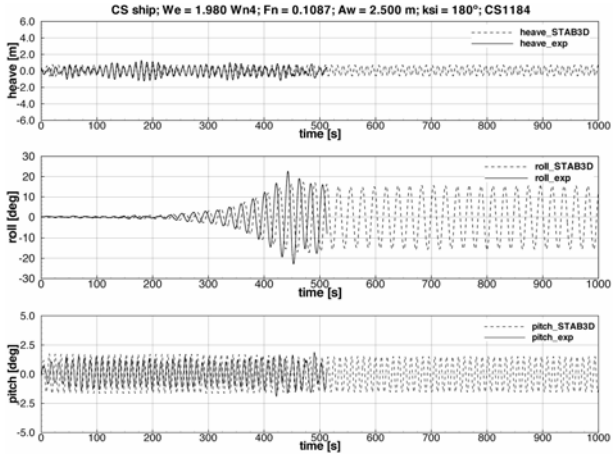

Fig. 11: Exp. 1184 ($\lambda / L = 1.00$). Parametric resonance occurs.

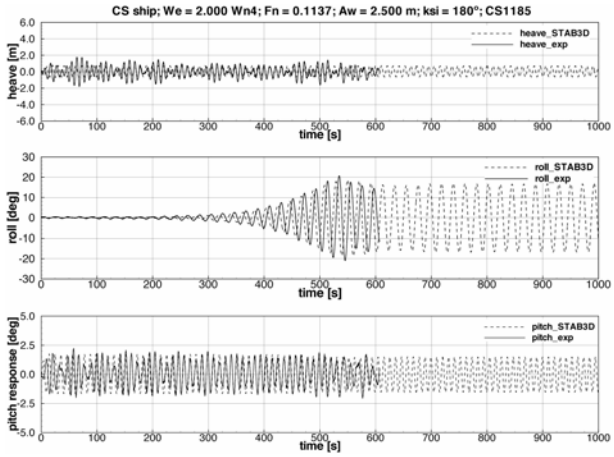

Fig. 12: Exp. 1185 ($\lambda / L = 1.00$). Parametric resonance occurs.

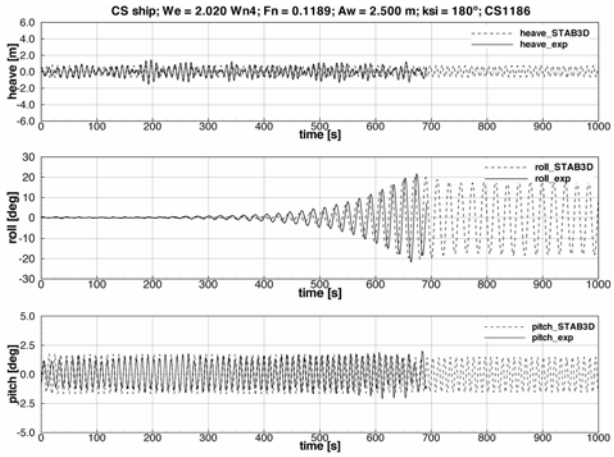

Fig. 13: Exp. 1186 ($\lambda / L = 1.00$). Parametric resonance occurs.

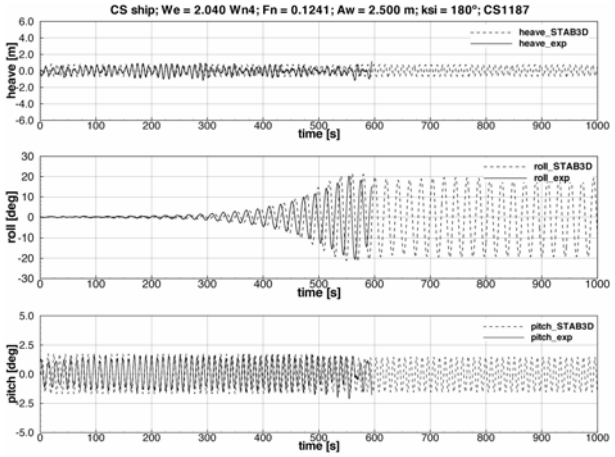

Fig. 14: Exp. 1187 ($\lambda / L = 1.00$). Parametric resonance occurs.

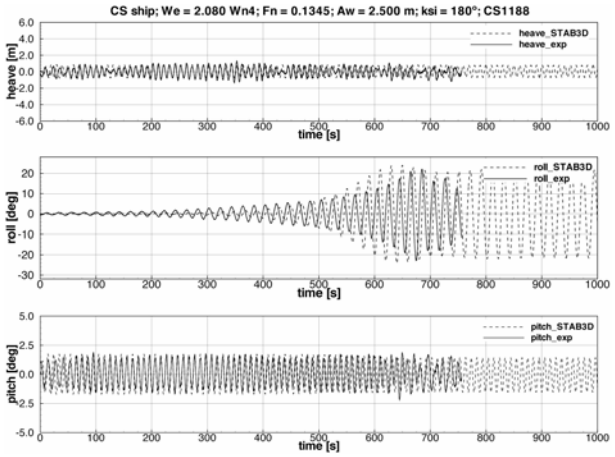

Fig. 15: Exp. 1188 ($\lambda / L = 1.00$). Parametric resonance occurs.

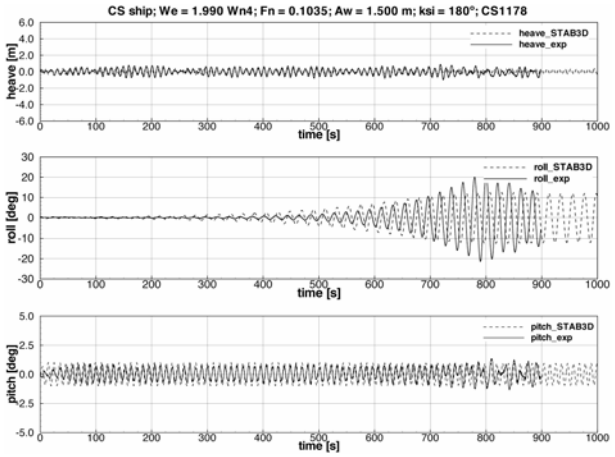

Fig. 16: Exp. 1178 ($\lambda / L = 0.97$). Parametric resonance occurs.

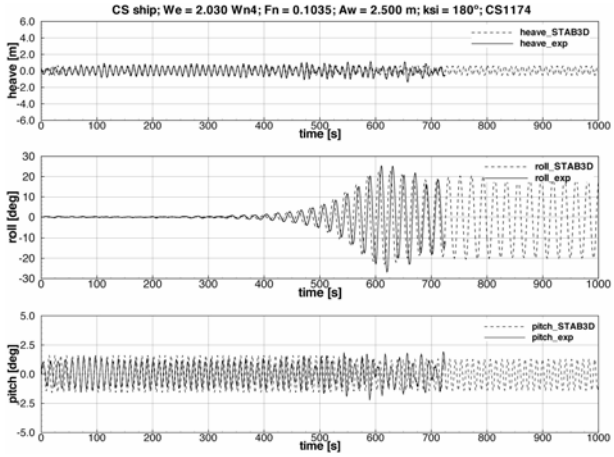

Fig. 17: Exp. 1174 ($\lambda / L = 0.95$). Parametric resonance occurs.

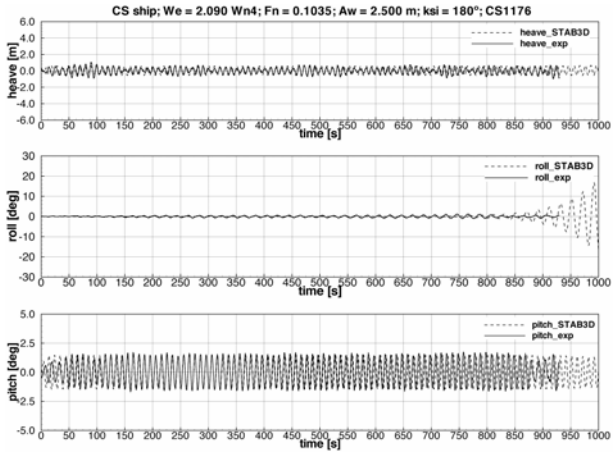

Fig. 18: Exp. 1176 ($\lambda / L = 0.90$). No parametric resonance.

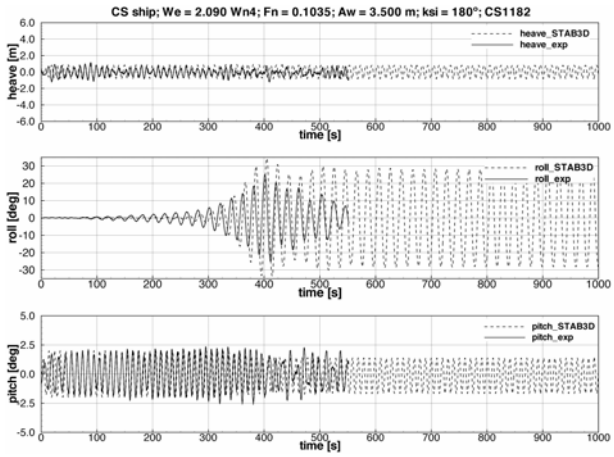

Fig. 19: Exp. 1182 ($\lambda / L = 0.90$). Parametric resonance occurs.

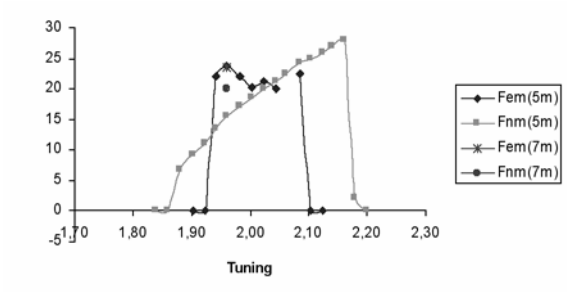

Fig. 20: Maximum roll amplitudes for $\lambda / L = 1$. Subscript e is experimental results, subscript n numerical. Number in parenthesis is wave height.

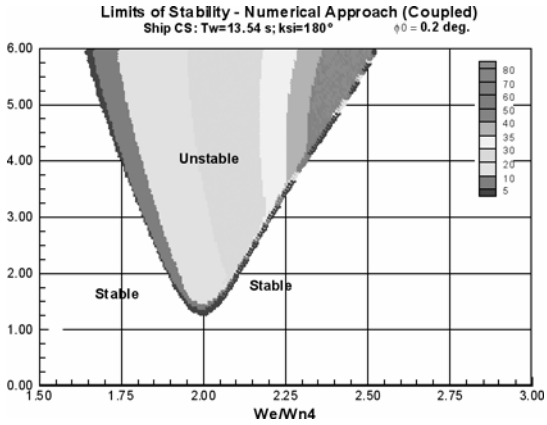

Fig. 21: Limits of stability for $\lambda / L = 1$.

CONCLUSIONS

A third order model for parametric resonance with coupling in roll-pitch-heave previously developed and validated with fishing vessels has been applied to a large container ship and validated showing good agreement with experimental and numerical results.

The accuracy of the model was best for heave and roll, while there was some discrepancy between experimental and numerical results for pitch for some conditions.

The model shows good agreement with the experimental results for roll in both experiments where parametric roll excitation occurred, and where it didn't occur. The range of encounter frequencies in which parametric excitation did occur is relatively wide. For these conditions the effects of tuning, speed and wave amplitude are clarified, as shown in Figures 20–21.

ACKNOWLEDGEMENTS

The present cooperative investigation is partially supported in Brazil by CNPq within the STAB project (Nonlinear Stability of Ships). The Brazilian authors also acknowledge financial support from LabOceano-COPPE/UFRJ and CAPES.

Thanks are due to UFRJ undergraduate student Vinicius L. Vileti, who ran a lot of simulations; to Luiz Cristóvão G. Coelho and Guilherme T. M. Alves from Intergraph-PUC, for the development of relevant parts of the computational code.

REFERENCES

Himeno, Prediction of ship roll damping — state of the art. Report No 239, Department of Naval Architecture and Marine Engineering, The University of Michigan 1981.

Neves, Rodríguez, A non-linear mathematical model of higher order for strong parametric resonance of the roll motion of ships in waves. Marine Systems & Ocean Technology, Sociedade Brasileira de Engenharia Naval 2005a

Neves, Rodríguez, A coupled third order model of roll parametric resonance. *Maritime Transportation and Exploration of Ocean and Coastal Resources*, p. 243-253 2005b.

Neves, Rodríguez, On unstable ship motions resulting from strong non-linear coupling. *Ocean Engineering*, 33:1853-1883 2006a.

Neves, Rodríguez, An Investigation on Roll Parametric Resonance in Regular Waves, Proceedings, 9th International Conference on Stability of Ships and Ocean Vehicles (STAB 2006), p 99-108 (Vol. 1), Rio de Janeiro, 2006b.

APPENDIX

Table A1 – Hydrostatic restoring coefficients (calm water): second order

Heave	Roll	Pitch
$Z_{zz} = -\frac{\partial^2 Z}{\partial z^2}$	$K_{zz} = 0$	$M_{zz} = -\frac{\partial^2 M}{\partial z^2}$
$Z_{z\phi} = 0$	$K_{z\phi} = -\frac{\partial^2 K}{\partial z \partial \phi}$	$M_{z\phi} = 0$
$Z_{z\theta} = -\frac{\partial^2 Z}{\partial z \partial \theta}$	$K_{z\theta} = 0$	$M_{z\theta} = -\frac{\partial^2 M}{\partial z \partial \theta}$
$Z_{\phi\phi} = -\frac{\partial^2 Z}{\partial \phi^2}$	$K_{\phi\phi} = 0$	$M_{\phi\phi} = -\frac{\partial^2 M}{\partial \phi^2}$
$Z_{\phi\theta} = 0$	$K_{\phi\theta} = -\frac{\partial^2 K}{\partial \phi \partial \theta}$	$M_{\phi\theta} = 0$
$Z_{\theta\theta} = -\frac{\partial^2 Z}{\partial \theta^2}$	$K_{\theta\theta} = 0$	$M_{\theta\theta} = -\frac{\partial^2 M}{\partial \theta^2}$

Table A2 – Hydrostatic restoring coefficients (calm water): third order

Heave		
$Z_{zzz} = -\frac{\partial^3 Z}{\partial z^3}$	$Z_{zz\phi} = 0$	$Z_{zz\theta} = -\frac{\partial^3 Z}{\partial z^2 \partial \theta}$
$Z_{z\phi\phi} = -\frac{\partial^3 Z}{\partial z \partial \phi^2}$	$Z_{\phi\phi\phi} = 0$	$Z_{\phi\phi\theta} = -\frac{\partial^3 Z}{\partial \phi^2 \partial \theta}$
$Z_{z\theta\theta} = -\frac{\partial^3 Z}{\partial z \partial \theta^2}$	$Z_{\phi\theta\theta} = 0$	$Z_{\theta\theta\theta} = -\frac{\partial^3 Z}{\partial \theta^3}$

Roll		
$K_{zzz}=0$	$K_{zz\phi}=-\frac{\partial^3 K}{\partial z^2\partial\phi}$	$K_{zz\theta}=0$
$K_{z\phi\phi}=0$	$K_{\phi\phi\phi}=-\frac{\partial^3 K}{\partial\phi^3}$	$K_{\phi\phi\theta}=0$
$K_{z\theta\theta}=0$	$K_{\phi\theta\theta}=-\frac{\partial^3 K}{\partial\theta^2\partial\phi}$	$K_{\theta\theta\theta}=0$

Pitch		
$M_{zzz}=-\frac{\partial^3 M}{\partial z^3}$	$M_{zz\phi}=0$	$M_{zz\theta}=-\frac{\partial^3 M}{\partial z^2\partial\theta}$
$M_{z\phi\phi}=-\frac{\partial^3 M}{\partial z\partial\phi^2}$	$M_{\phi\phi\phi}=0$	$M_{\phi\phi\theta}=-\frac{\partial^3 M}{\partial\phi^2\partial\theta}$
$M_{z\theta\theta}=-\frac{\partial^3 M}{\partial z\partial\theta^2}$	$M_{\phi\theta\theta}=0$	$M_{\theta\theta\theta}=-\frac{\partial^3 M}{\partial\theta^3}$

Heave-roll-pitch coupling		
$Z_{z\phi\theta}=0$	$K_{z\phi\theta}=-\frac{\partial^3 K}{\partial z\partial\phi\partial\theta}$	$M_{z\phi\theta}=0$

Table A3 – Derivatives due to wave passage: second order

$Z_{\zeta z}(t)=-\frac{\partial F_3^{FK(1)}}{\partial z}$	$K_{\zeta z}(t)=0$	$M_{\zeta z}(t)=-\frac{\partial F_5^{FK(1)}}{\partial z}$
$Z_{\zeta\phi}(t)=0$	$K_{\zeta\phi}(t)=-\frac{\partial F_4^{FK(1)}}{\partial\phi}$	$M_{\zeta\phi}(t)=0$
$Z_{\zeta\theta}(t)=-\frac{\partial F_3^{FK(1)}}{\partial\theta}$	$K_{\zeta\theta}(t)=0$	$M_{\zeta\theta}(t)=-\frac{\partial F_5^{FK(1)}}{\partial\theta}$

Table A4 – Derivatives due to wave passage: third order

Heave		
$Z_{\zeta\zeta z}(t)=-\frac{\partial F_3^{FK(2)}}{\partial z}$	$Z_{\zeta\zeta\phi}(t)=0$	$Z_{\zeta\zeta\theta}(t)=-\frac{\partial F_3^{FK(2)}}{\partial\theta}$
$Z_{\zeta zz}(t)=-\frac{\partial^2 F_3^{FK(1)}}{\partial z^2}$	$Z_{\zeta z\phi}(t)=0$	$Z_{\zeta z\theta}(t)=-\frac{\partial^2 F_3^{FK(1)}}{\partial z\partial\theta}$
$Z_{\zeta\phi\phi}(t)=-\frac{\partial^2 F_3^{FK(1)}}{\partial\phi^2}$	$Z_{\zeta\phi\theta}(t)=-\frac{\partial^2 F_3^{FK(1)}}{\partial\theta^2}$	$Z_{\zeta\phi\phi}(t)=0$

Roll		
$K_{\zeta\zeta z}(t)=0$	$K_{\zeta\zeta\phi}(t)=-\frac{\partial F_4^{FK(2)}}{\partial\phi}$	$K_{\zeta\zeta\theta}(t)=0$
$K_{\zeta zz}(t)=0$	$K_{\zeta z\phi}(t)=-\frac{\partial^2 F_4^{FK(1)}}{\partial z\partial\phi}$	$K_{\zeta z\theta}(t)=0$
$K_{\zeta\phi\phi}(t)=0$	$K_{\zeta\phi\theta}(t)=0$	$K_{\zeta\phi\theta}(t)=-\frac{\partial^2 F_4^{FK(1)}}{\partial\phi\partial\theta}$

Pitch		
$M_{\zeta\zeta z}(t)=\frac{\partial F_5^{FK(2)}}{\partial z}$	$M_{\zeta\zeta\phi}(t)=0$	$M_{\zeta\zeta\theta}(t)=\frac{\partial F_5^{FK(2)}}{\partial\theta}$
$M_{\zeta zz}(t)=\frac{\partial^2 F_5^{FK(1)}}{\partial z^2}$	$M_{\zeta z\phi}(t)=0$	$M_{\zeta z\theta}(t)=-\frac{\partial^2 F_5^{FK(1)}}{\partial z\partial\theta}$
$M_{\zeta\phi\phi}(t)=-\frac{\partial^2 F_5^{FK(1)}}{\partial\phi^2}$	$M_{\zeta\phi\theta}(t)=-\frac{\partial^2 F_5^{FK(1)}}{\partial\theta^2}$	$M_{\zeta\phi\theta}(t)=0$